Open access • Journal Article • DOI:10.1080/14786430412331309344

Rumpling instability in thermal barrier systems under isothermal conditions in vacuum — Source link

Rahul Panat, K. Jimmy Hsia, Joseph W. Oldham

Institutions: University of Illinois at Urbana–Champaign

Published on: 01 Jan 2005 - Philosophical Magazine (Taylor & Francis Group)

Topics: Aluminide, Nickel aluminide and Thermal barrier coating

Rumpling instability in thermal barrier systems under isothermal conditions in vacuum

Rahul Panat, K. Jimmy Hsia* and Joseph Oldham
Department of Theoretical and Applied Mechanics
University of Illinois, Urbana, IL 61801,USA

Abstract

Bond coat (BC) surface rumpling has been identified as one of the important mechanisms that can lead to failure of the thermal barrier coatings. The driving force behind rumpling – whether the stresses in the thermally grown oxide over the BC or the stresses in the BC – remains to be clarified. Meanwhile, the mass transport mechanisms in the BC leading to rumpling are not clearly identified. In the present investigation, we subject two types of BC-superalloy systems, nickel aluminide and platinum aluminide BCs on a Ni-based superalloy, to isothermal exposure at temperatures ranging from 1150 °C to 1200 °C in vacuum. The results show that the nickel aluminide BC rumples at 1200 °C and at 1175 °C in absence of significant oxidation. The wavelength of the rumpled surfaces was 60-100 μm, with an amplitude of 5-8 μm. The rumpling was insensitive to the initial BC surface morphology. At 1150 °C, no clear rumpling was observed, but some surface undulations could be seen related to the BC grains. The platinum aluminide BC with an initially polished surface showed the formation of dome like structures corresponding to the BC grains at 1200 °C, indicating a strong influence of BC grain boundary diffusion on the BC rumpling. The above observations indicate that a large scale mass transport manifested in the form of BC rumpling can occur in absence of a significant oxide layer. The stresses in the BC appear to be sufficient to cause the rumpling behavior. The current rumpling results are discussed in the context of the possible mechanisms. It is concluded that various diffusive processes (grain boundary, surface and bulk diffusion) in the BC driven by the BC stresses lead to the rumpling behavior observed in the current study.

*Corresponding author. Email: kjhsia@uiuc.edu, Fax: 1(217) 244 5707.

Keywords: Thermal Barrier Coatings; Surface Rumpling; Surface Diffusion; Grain Boundary Diffusion; Thermally Grown Oxide; Deformation Mechanisms

1 INTRODUCTION

Thermal barrier coatings (TBCs) have been developed to boost the performance of gas turbines, jet engines, and diesel engines (Goward, 1998; Meier & Gupta, 1994; Miller, 1987; Padture *et al.*, 2002; Schulz *et al.*, 2003; Sheffler & Gupta, 1988; Stiger *et al.*, 1999; Strangman, 1985). The TBCs are multi-layered structures that help reduce the temperature of the hot components in these applications, resulting in an improved efficiency, or equivalently, the component creep life in these applications. A TBC system consists of: (i) a ceramic top layer that provides the required temperature gradient, (ii) an intermediate (metallic) bond coat (BC) deposited on the base superalloy to enhance the TBC oxidation resistance and improve the adherence of the ceramic top layer, and (iii) a thermally grown oxide (TGO) that forms over the BC surface at the BC-ceramic interface and continuously evolves at high temperature.

One of the problems limiting the use of TBCs is the ceramic topcoat spallation after certain amount of thermal exposure. The topcoat spallation is quite dangerous since the local operating temperatures in the gas turbine hot sections can exceed the melting temperature of the superalloy substrate. The TBC failure problem has been investigated under isothermal, thermomechanical or cyclic thermal histories (Ali *et al.*, 2002; Ambrico *et al.*, 2001; Bartlett & Maschio, 1995; Bartsch *et al.*, 2003, 2001; Baufeld *et al.*, 2001; Bose & Demasi-Marcin, 1997; Bouhanek *et al.*, 2000; Busso *et al.*, 2001; Clarke & Shillington, 1999; Ibegazene-Ouali *et al.*, 2000; Kim *et al.*, 2002; McDonald & Hendricks, 1980; Miller & Lowell, 1982; Ruud *et al.*, 2001; Schulz *et al.*, 2001; Tolpygo & Clarke, 2001; Tolpygo *et al.*, 2001; Vaidyanathan *et al.*, 2000; Wright, 1998; Wu *et al.*, 1989). The TBC failure is seen to vary from system to system (Bouhanek *et al.*, 2000; Ruud *et al.*, 2001; Schulz *et al.*, 2001; Tolpygo & Clarke, 2001; Tolpygo *et al.*, 2001). One of the significant indications from these studies is that the failure process is related to instabilities occurring at BC-ceramic interface, with the TGO in between (Evans *et al.*, 2001; Wright & Evans, 1999). One such instability is the BC surface "rumpling", or progressive roughening of the BC surface to characteristic wavelengths in the BC-superalloy systems upon thermal cycling (Deb *et al.*, 1987; Holmes & McClintock, 1990; Panat & Hsia, 2003a; Pennefather & Boone,

1995; Tolpygo & Clarke, 2000; Zhang *et al.*, 1999). The rumpling instability in presence of the ceramic topcoat creates a geometric incompatibility in the form of cracks at the BC (or TGO)-ceramic interface and contribute to the cause of TBC failure (Baufeld & Barstch, 2003; Mumm *et al.*, 2001; Tolpygo & Clarke, 2000, 2001). This instability is shown to be 'suppressed' under certain circumstances, e.g. when the TGO-ceramic interface remains intact (Tolpygo & Clarke, 2001). The suppression of rumpling can, however, give rise to residual stresses at the BC-TGO interface and contribute to other TBC failure processes (e.g. BC-TGO separation). This necessitates a thorough understanding of the mechanisms of BC rumpling.

Several experimental (Deb *et al.*, 1987; Holmes & McClintock, 1990; Panat & Hsia, 2003a; Pennefather & Boone, 1995; Tolpygo & Clarke, 2000; Zhang *et al.*, 1999) and theoretical (Balint & Hutchinson, 2003; He *et al.*, 2000; Karlsson & Evans, 2001; Panat *et al.*, 2003; Suo, 1995; Tolpygo & Clarke, 2000) studies have been carried out to address the BC rumpling. Platinum aluminide, nickel aluminide and NiCoCrAlY BCs deposited on superalloy substrates were shown to rumple to wavelengths ranging from 30-50 μm (Tolpygo & Clarke, 2000) to about 300 μm (Pennefather & Boone, 1995) upon thermal cycling to temperatures up to 1200 °C in air. The amplitude of rumpled surfaces in these experiments was up to 15 μm. Under very fast heating and cooling rates (1050°C to 300°C temperature change in less than a minute) along with mechanical loading of the superalloy substrate, the BCs did (Holmes & McClintock, 1990; Zhang *et al.*, 1999) or did not (Busso & McClintock, 1993) show rumpling. Other effects related to thermal shock were observed in these experiments such as "scalloping" (Holmes & McClintock, 1990), i.e., large scale spallation of the TGO and formation of highly elliptical voids (Busso & McClintock, 1993). Under isothermal experiments at 1100 °C (Deb *et al.*, 1987; Panat & Hsia, 2003a) and at 1150 °C (Tolpygo & Clarke, 2000), no rumpling was observed, while at 1175 °C and at 1200 °C BC was seen to rumple (Panat & Hsia, 2003a). Suo *et al.* (2003) found extensive void formation below the TGO after 300 hour isothermal exposure in air at 1150 °C.

To understand the BC rumpling phenomenon, one needs to address two important issues, viz, the driving force for rumpling and the mass transport mechanisms that lead to the rumple formation. According to He *et al.* (2000) and Karlsson & Evans (2001), the plastic ratcheting of the BC due to the thermal mismatch stresses in the developing TGO during thermal cycling can cause rumpling. Suo (1995) on the other hand has suggested that the highly compressive growth stresses in the TGO (on the order of GPa) would provide the driving force necessary for the metal atoms to diffuse

along the TGO-metal interface, leading to a wavy metal surface. In a recent model, Balint & Hutchinson (2003) have shown that the compressive stresses in the TGO along with the stresses in the BC can lead to rumpling under the conditions of the BC undergoing power-law creep (dislocation creep). The above models are generic to metal-oxide systems and require the existence of highly stressed TGO for rumpling to occur. Tolpygo & Clarke (2000) have speculated that the rumpling in the BC-superalloy systems occurs as a result of differential diffusion of various constituents such as Ni and Al, perpendicular to the BC surface. The model by Panat *et al.* (2003) is based on the assumption that the stresses in BC provide the necessary driving force for rumpling. A balance between the strain energy density at the BC surface and the BC surface energy would then decide the characteristic rumple wavelength. The mechanism they (Panat *et al.*, 2003) proposed was the surface diffusion of BC atoms at the BC-TGO interface.

Thus, the possible deformation mechanisms of rumpling include: 1) cyclic plastic ratcheting of the BC driven by the stresses in the TGO, 2) Dislocation creep in the BC driven by the stresses in the TGO and the BC, 3) diffusive processes in the BC driven by the material concentration gradients in the BC cross-section, and 4) diffusive processes in BC driven by the stresses in the BC or in the TGO. Note that the sources of the stresses in the TGO include its thermal mismatch with the BC (He *et al.*, 2000; Tolpygo & Clarke, 2000) and its own growth at high temperatures (Suo, 1995), while those for BC include its thermal mismatch with the superalloy substrate (Karlsson & Evans, 2001; Panat *et al.*, 2003; Watanabe *et al.*, 2002) and the phase transformations occurring in the BC at 650-700 °C (Chen *et al.*, 2003). Also, possible diffusive processes in BC driven by the BC stress include surface diffusion, bulk diffusion and grain boundary diffusion.

The current experimental investigation is based on the desire to clarify the driving force and the kinetics governing the rumpling processes in BC-superalloy systems. We carry out isothermal experiments at various temperatures up to 1200 °C in vacuum on platinum aluminide and nickel aluminide BCs deposited on René N5, a Ni-based superalloy. The nickel aluminde BC is shown to form clear rumples in absence of significant oxidation. The BC grains and the BC microstructure in this case were not seen to influence the rumpling behavior. The platinum aluminide BC is shown to rumple at high temperatures, with the undulations correlated with the BC grains. It is shown that a micron-scale mass transport due to diffusive processes in the BC driven by the BC stresses can result in the observed rumpling. These diffusive pro-

cesses include the grain boundary diffusion, surface diffusion or bulk diffusion, or a combination of these processes.

2 EXPERIMENTAL PROCEDURE

The superalloy substrate used in the present study was René N5, a Ni-based superalloy supplied by the General Electric Aircraft Engines (Cincinnati, OH, USA). The BCs were deposited on the superalloy by Chromalloy Gas Turbine Corporation (Orangeburg, NY, USA). The platinum aluminide BC deposition process involved electroplating a Pt layer on the superalloy followed by a vacuum heat treatment and a vapor phase aluminization. The nickel aluminide BC was deposited on the superalloy substrate by vapor phase aluminization. The test samples were approximately, 5 mm $\times$ 5 mm $\times$ 3 to 5 mm in dimension.

The nickel aluminide BCs were subjected to isothermal exposure at 1150 °C, 1175 °C and 1200 °C. The surfaces of these BCs were in as-received condition or were polished using diamond paste to partially or completely remove the initial surface undulations. The platinum aluminide BC surfaces were polished down to 1 μm diamond paste and subjected to 1175 °C and 1200 °C. Some platinum aluminide BC specimens with as-deposited surface were also subjected to isothermal exposure at 1200 °C. The hold times for the experiments were 25 hours and 50 hours. The times and temperatures of exposure as well as the initial BC surface conditions were chosen to capture the important features of the behavior of these coatings at high temperatures in vacuum.

A tube furnace (HTF55322A, Lindberg/Blue M, Asheville, NC, USA) along with a quartz tube carrying the BC-superalloy specimens was used for the experiments. The tube was connected to a roughing pump/diffusion pump assembly to produce a vacuum level up to 10^{-8} torr at 1200 °C. In some experiments, the vacuum level was seen to fall occasionally to about 10^{-6} torr. The furnace provided a linear heating rate of about 22 °C per minute for all the experiments. The samples were furnace cooled at the end of the hold time for each of the experiments. The specimen temperature was measured using a K-type thermocouple (Omega, Stamford, CT, USA) calibrated by an optical pyrometer (The Pyrometer Instrument Company Inc., Northvale, NJ). The estimated error in the temperature measurement was about $\pm$ 0.75 % when measured in °C. Some of the samples were cut and their cross section polished successively down to 1 μm diamond paste to observe the microstructural changes. The samples

were examined using profilometry, scanning electron microscopy (SEM), the semi quantitative elemental analysis tool of energy dispersive X-ray spectroscopy (EDX), X-ray photoelectron spectroscopy (XPS), and Augur electron spectroscopy (AES).

3 RESULTS

3.1 Initial Microstructure and Composition

Figure 1 shows the representative SEM images of the cross-section and top views of the as-received nickel aluminide BC (Figs. 1a,c) and the platinum aluminide BC (Figs. 1b,d). The corresponding profilometer scans can be seen in Fig. 1e and Fig. 1f, respectively. The composition of nickel aluminide BC is (wt%) 13.7Al-6Cr-7.8Co-bal Ni, while that of the platinum aluminide BC is (wt%) 17Al-7Cr-9Co-40Pt-bal Ni as determined by EDX analysis. Both BCs show a two-layered structure consisting of an outer zone (label '1') and an interdiffusion zone, or IDZ (label '2'). The IDZ of both BCs contains precipitates (bright regions in Figs. 1a,b) rich in refractory elements, viz, W, Mo, and Ta. Alumina inclusions, shown by black arrows in Figs. 1a,b, are irregularly placed at the border between region 1 and region 2. The BC compositions in the outer zones of the two BCs varied slightly in the direction perpendicular to the BC surface. For nickel aluminide BC, the Al content decreased from top (about 18 wt%) to the IDZ (about 11 wt%), with a concomitant rise in the Co and Cr content. For the platinum aluminide BC, the Al content decreased from top (about 22 wt%), to the IDZ (about 15 wt%) with a similar increase in the Co and Cr content. The nickel aluminide and the platinum aluminide BC grains can be seen in Figs. 1c and 1d, respectively. The grain size for the nickel aluminide BC is about 20 μm while that for platinum aluminide BC is about 30-50 μm. The composition of the René N5 superalloy (from Walston *et al.*, 1996) is (wt%) 7.5Co-7Cr-1.5Mo-6.5Ta-5W-3Re-6.2Al-0.15Hf-0.05C-0.004B-0.01Y-bal Ni.

3.2 Isothermal exposure in vacuum: Nickel aluminide BC

Figure 2 shows the nickel aluminide BC surface (Figs. 2a,c) and the corresponding profilometer scan (Fig. 2b) after an isothermal exposure in vacuum at 1200°C for 25 hours. Clearly, the surface has developed rumples with a wavelength of 60-100 μm and an amplitude of 5-8 μm. This range of wavelengths and amplitude is comparable to that observed in literature (Deb *et al.*, 1987; Holmes & McClintock, 1990; Panat

et al., 2003; Tolpygo & Clarke, 2000) during cycling and isothermal experiments on BCs in air. In Fig. 2c, the BC grain boundaries are seen in addition to the BC rumples. Although a few BC grain boundaries were aligned along the rumple valleys, it is apparent that there is little correlation between the BC grains and the waviness. The difference in the periodicity of the rumples (Fig. 2b) and the BC grain size (Fig. 2c) confirms this conclusion. The rumpling seen in Fig. 2c has a local directionality, a feature also observed for platinum aluminide BCs under thermal cycling (Panat & Hsia, 2003a; Tolpygo & Clarke, 2000). The reason for this phenomenon is not known at present, but it possibly happens due to local anisotropy in the BC material characteristics.

To estimate the thickness of the oxide layer developed over the BC, we use the method proposed by Strohmeier (1990) and Finnie *et al.* (2000). An XPS spectrum representing Al 2p peak envelop of the BC surface is obtained as shown in Fig. 3. The binding energies of the peaks representing Al metal and Al oxide are sufficiently apart to get the individual areas under the peaks (Fig. 3). Since the TGO over the BC surfaces is an Al oxide, the areas computed under these peaks can be utilized to estimate the oxide layer thickness (Finnie *et al.*, 2000; Strohmeier, 1990). Although this method is used to obtain the thickness of Al oxide over a pure Al metal, it can also be used for an *estimate* of oxide thickness over an Al alloy by assuming that the metals other than Al are replaced by Al. The ratio of the areas under the peaks representing the Al metal and the Al oxide is (from the curve-fit in Fig. 3) about 1/6.3. This gives the oxide thickness of about 1.7 nm (Finnie *et al.*, 2000) or 2.3 nm (Strohmeier, 1990). Thus, it is concluded that the oxide layer over the BC is only about a few nanometers thick, close to the native oxide thickness for Al (Saif *et al.*, 2002).

Fig. 4 shows an SEM micrograph (with backscatter electrons) of the the cross-section of the rumpled sample in Fig. 2, revealing several interesting features formed after the thermal treatment in vacuum. The BC grain boundaries are revealed in the cross-section as the brighter regions seen due to chemical composition changes as indicated in the high magnification micrograph of Fig. 4. Large bright regions indicated by "n" can also be seen along the grain boundaries where aluminum was depleted (about 5 wt % Al) when compared to the BC matrix (about 11 wt% Al). The composition of the grain boundaries was identical to that of these bright regions. The overall loss of Al in the BC in absence of oxidation can be attributed to its diffusion to the superalloy at high temperatures (Tolpygo & Clarke, 2000). Alumina inclusions

(denoted by "m") are seen as the dark regions in the higher magnification micrograph of Fig. 4. These alumina inclusions were present before the isothermal exposure as shown in Fig. 1a. The IDZ of the BC has developed random precipitates (denoted by "p") rich in W, Mo and Ta. These precipitates, when compared to the as-deposited condition (Fig. 1a), have undergone considerable coarsening and agglomeration upon high temperature exposure. The BC also shows considerable increase in thickness when compared to the as-deposited condition in Fig. 1. The visibility of the BC grains in Fig. 2c is due to extensive faceting of the BC surface developed upon the thermal treatment in vacuum as shown in Fig. 5. Figure 5 shows that the facets along the grain boundaries and the interior of grains have a periodicity of about 200-300 nm. Interestingly, the BC has developed a waviness of tens of micrometers, essentially unaffected by these smaller scale features. Note that the directionality of these features was different for different BC grains.

To assess the effect of initial surface roughness on waviness formation, a nickel aluminide BC sample was polished down to 1 μm diamond paste and subjected to isothermal exposure for 50 hours at 1200 °C in vacuum. Figures 6(a,b) show the initial surface of the BC and the corresponding profilometer scan. The initial BC surface undulations in Fig. 6(b) are about 30-40 nm in amplitude (peak to valley distance). After the isothermal exposure, the BC surface rumpled with an amplitude of about 4 μm, a two orders of magnitude increase as shown in Fig. 6(c,d). The inset in Fig. 6c shows the rumpling and the BC grains with no apparent correlation between the two, similar to the sample shown in Fig. 2.

The results of thermal exposure at 1175 °C and 1150 °C are shown in Fig. 7. Figure 7a shows the BC surface after 50 hour thermal exposure at 1175 °C. This surface topography is quite similar to that for the specimen exposed to 1200 °C as seen in Fig. 2b. At this slightly lower temperature, however, some of the BC grain boundaries can be seen to correlated with the rumpling ridges. At 1150 ° after 25 hour exposure, the BC surface shows no clear long-range rumpling, but small fluctuations correlated with the grain boundaries can be observed over the surface (Fig. 7b).

3.3 Isothermal exposure in vacuum: Platinum aluminide BC

Figure 8 shows the surface morphology of a platinum aluminide BC before (Fig. 8a) and after (Fig. 8b,c) 50 hour thermal exposure at 1200 °C in vacuum. Clearly, upon isothermal exposure, the initial polished surface with fluctuations of about 20 nm in amplitude (Fig. 8a) developed a rumpled surface with an amplitude of fluctuation

of about 5-7 μm (Fig. 8b,c). This two orders of magnitude increase in amplitude is similar to that for the nickel aluminide BC shown in Fig. 6. Unlike the nickel aluminde BC, however, the rumpling of the platinum aluminide BC was closely correlated with the BC grains; the grain boundaries being "depressed", while the grain interiors being "elevated". The grain interior and boundary structures can be seen in the high resolution SEM micrographs of the same BC surface in Fig. 9. Extensive faceting developed over the BC grain surfaces and along the grain boundaries. Note that these facets have a periodicity of about 100 - 200 nm, similar to that for the rumpled nickel aluminide BC (Fig. 5).

The thickness of the oxide layer over the platinum aluminide BC could not be estimated using the XPS method (Finnie *et al.*, 2000; Strohmeier, 1990) due to the Al 2p peaks being overlapped by the Pt 4f peaks. We used AES to obtain the elemental composition as a function of depth over the platinum aluminide BC surface (Fig. 8b) as shown in Fig. 10 to measure the oxide thickness. Argon ions at 3 KeV were used to sputter (remove) the surface material successively. The measurement was found to be repeatable on different platinum aluminide BC grain interiors. From Fig. 10, significant signal attributed to Ni and Pt can be observed at a depth greater than about 2 nm. At the same time, the oxygen decreases with sputter depth, corresponding to the removal of the oxide. The error in the measurement is less than about ± 2.5 nm corresponding to the inelastic mean free path of Auger electrons before escaping a surface. Clearly, the oxide thickness for the platinum aluminide BC is less than 5 nm, comparable to that over the nickel aluminide BC.

Fig. 11 shows an SEM micrograph (with backscatter electrons) of the the cross-section of the rumpled sample in Fig. 8, revealing features quite similar to that for the nickel aluminide BC (Fig. 4). Large bright regions indicated by "r" can also be seen where aluminum was depleted (about 7 wt % Al) when compared to the BC matrix (about 15 wt% Al). The overall loss of Al in the BC in absence of TGO can again be attributed to its diffusion to the superalloy at high temperatures (Tolpygo & Clarke, 2000). Unlike the nickel aluminide BC, the platinum aluminide BC grain boundaries were not revealed in the cross-section even with the contrast of the backscatter electrons. Alumina inclusions (denoted by "q") are seen as the dark regions in the higher magnification micrograph of Fig. 11. These alumina inclusions were present before the isothermal exposure as shown in Fig. 1b. An isolated void can be seen in the BC cross-section as shown by black arrow in Fig. 11. The IDZ of the BC has developed precipitates (denoted by "s") rich in W, Mo and Ta. These precipitates,

similar to the nickel aluminide BC (Fig. 4), have undergone considerable coarsening and agglomeration upon high temperature exposure. The BC has also shown an increase in thickness when compared to the as-deposited condition (Fig. 1b). The increase in the BC thickness and the coarsening of the refractory rich precipitates upon high temperature exposure for the two BCs (Figs. 4 and 11) has been observed during BC thermal cycling and isothermal exposure in air (Busso & McClintock, 1993; Holmes & McClintock, 1990; Panat & Hsia, 2003a; Tolpygo & Clarke, 2000). Such a phenomenon is attributed to the diffusion of Ni from the superalloy to the BC at high temperature and the subsequent decrease of the solubility of refractory elements of the superalloy below the BC-substrate interface (Busso & McClintock, 1993; Holmes & McClintock, 1990).

In several observations at high temperatures (1150 °C, 1175 °C and 1200 °C), clear rumpling could not be seen since the platinum aluminide BCs formed a non-uniform oxide layer over the surface. The platinum aluminide BC surface may develop isolated oxide sites and undulations with a periodicity of about 20 μm, smaller than that without any oxide formation. Note that in ambient air, a continuous oxide layer is formed over the platinum aluminide BC at high temperatures (Panat & Hsia, 2003a; Tolpygo & Clarke, 2000).

Table 1 summarizes all the experimental results presented in section 3.

4 DISCUSSION

The experimental results in the current study have shed light on clarifying the driving force for rumpling and identifying possible rumpling mechanisms. We have shown that mass transport leading to micron-scale deformations manifested in the form of rumpling can occur in the BC-superalloy systems in absence of a significant oxide layer. Also, the rumpling is shown to occur under isothermal conditions depending upon the temperature of testing. In the present section, we discuss the possible driving forces and the kinetics of rumpling.

4.1 Driving Force

The prevailing view of many researchers states that the thin TGO under highly compressive stress provides the driving force for BC surface rumpling (Balint & Hutchinson, 2003; He *et al.*, 2000; Karlsson & Evans, 2001; Suo, 1995) since such thin layer has a tendency to buckle. In the present study, we demonstrate that rumpling oc-

curred in the BC-superalloy systems even when the oxide layer over the BC was of insignificant thickness (e.g. Fig. 2 and Fig. 8). Clearly, this native oxide (a few nanometers thick) should not be the cause of the BC rumpling. This leaves the possibility of the concentration gradients in the BC (Tolpygo & Clarke, 2000), or the stresses in the BC (Panat *et al.*, 2003) as the possible driving force for rumpling. Figure 4 shows that the periodicity of the refractory rich precipitates (indicated by "p") does not match that of the rumples, neither do the aluminum depleted zones that are irregularly placed as shown in Fig. 4 (denoted by "n"). Similarly, the aluminum depleted zones and the refractory rich regions of the platinum aluminide BC cross section (Fig. 11) do not show a periodicity corresponding to the platinum aluminide surface undulations (Fig. 8). Furthermore, we did not observe any void formation in the nickel aluminide BCs upon isothermal exposure. Isolated voids formed in the platinum aluminide BC did not correspond with the rumples. It is clear that the material concentration changes in the BC cross section show a poor correlation with the BC rumples. Similar conclusion was drawn about the role of the microstructure in inducing BC surface instabilities for platinum aluminide BC-superalloy system both in presence (Mumm *et al.*, 2001) and in absence (Panat & Hsia, 2003a) of the ceramic topcoat in air.

This leaves us with the only viable alternative, i.e., *the stresses in the BC alone are capable of inducing BC rumpling* in nickel aluminide and platinum aluminide BC-superalloy systems under current testing conditions. The origin of the BC stresses are believed to be the thermal mismatch between the BC material and the substrate, and possibly phase transformation (Chen *et al.*, 2003; Karlsson & Evans, 2001; Panat *et al.*, 2003; Watanabe *et al.*, 2002). Therefore, the magnitude of this driving force depends on how far the testing temperature is from the BC deposition temperature (Panat & Hsia, 2003a,b). Under different testing conditions, e.g., in air, the formation of TGO may potentially influence the rumpling behavior. However, the present study shows that the characteristic wavelength and the amplitude of rumpled BC surface tested in vacuum are comparable to those tested in air (Deb *et al.*, 1987; Panat & Hsia, 2003a; Tolpygo & Clarke, 2000), indicating a limited role by TGO under isothermal heating.

4.2 Governing Kinetics

The fact that rumpling can occur under isothermal conditions indicates that cyclic plasticity, i.e., ratcheting of the BC (He *et al.*, 2000) is not necessarily the dominant

mechanism for rumpling. Although the exact role of the BC ratcheting on BC rumpling under other testing conditions is not known, it is likely to play a secondary role during rumpling even under thermal cycling (Panat & Hsia, 2003a). Further, the material concentration changes in the BC cross-section have a poor correlation with the rumples, indicating that concentration driven BC diffusion (Tolpygo & Clarke, 2000) would not govern the kinetics of the rumpling seen in the current study. The recently suggested creep mechanism by Balint & Hutchinson (2003) is a plausible mass transport mechanism for BC surface rumpling. The small scale faceting seen in Fig. 5 seems to lend support to such dislocation creep mechanism during BC rumpling. However, their model requires the presence of stressed TGO to provide the driving force, which is not the case in the current study. Nevertheless, BC stress induced creep deformation may potentially give rise to a rumpled surface.

Other kinetic processes include diffusive mechanisms such as surface diffusion, volume diffusion, and grain boundary diffusion. The BC stress driven surface diffusion model by Panat *et al.* (2003) can explain several experimental results of the nickel aluminide BC rumpling in the current study. Figures 2 and 6 show that the rumpling phenomenon is relatively insensitive to the initial surface fluctuations as predicted by the model (Panat *et al.*, 2003). Further, this model predicts that the rumpling under isothermal conditions in absence of any oxide layer can occur, as observed in the current study. It is noted, however, that the model by Panat *et al.* (2003) only takes into account the surface diffusion mechanism, and does not take into account other diffusion mechanisms such as volume diffusion through the BC bulk and grain boundary diffusion (Mullins, 1963; Shewmon, 1989; Thouless, 1993). New modelling efforts are being pursued to take into account all the significant diffusive processes in the BCs to predict the rumpling behavior (Panat & Hsia, 2003b). The fact that the rumpling is correlated with the grain structures in platinum aluminide BC points to the possibility that grain boundaries are an additional diffusion path during rumpling. The difference in the dominant paths of diffusion in the case of the nickel aluminide and the platinum aluminide BCs is not currently known. We speculate a competition between grain boundary diffusion and the BC volume diffusion depending upon the testing temperature (Shewmon, 1989). This competition arises due to the lower activation energy of grain boundary diffusion compared to that of the volume diffusion. At moderate temperatures, the grain boundary diffusion forms the high diffusivity path. But as the temperature increases, volume diffusion becomes dominating over grain boundary diffusion. Thus, a combination of BC volume diffusion and surface

diffusion would decide the rumpling process at higher temperatures, while at lower temperatures, grain boundary diffusion should be observed. Qualitatively, we see that at 1200 °C, the BC surface undulations are not related to the grain structure (Fig. 2). But at 1175 °C and at 1150 °C an increased correlation between the two is seen (Figs. 7b,d). Unfortunately, the grain boundary diffusivity has not been measured in the BC-superalloy systems. We also do not have quantitative information on the BC surface diffusion. To fully identify the dominant mechanism(s), a study aimed at measuring various diffusion constants in the BC-superalloy systems at different temperatures needs to be carried out.

The processes leading to the rumpling in the case of platinum aluminide BC shown in Fig. 8 could be a combination of surface and grain boundary diffusion. Such a process has been modelled by Thouless (1993) for an array of grains under a remote stress. His analysis shows that a combination of grain boundary diffusion and surface diffusion would give rise to the surface morphologies similar to those seen in Figs. 8 and 9. Again, for any comparison, the diffusivity of platinum aluminide BC along various diffusion paths needs to be measured at various temperatures.

The results presented in the current study have important implications to the TBC failure process. Our main objective here is to identify the role of the BC stresses and the diffusive processes in the BC in TBC failure. These stresses appear to be important in the evolution of TBC systems during high temperature exposure. Different diffusive processes in the BC could lead to surface rumpling of several micrometers in amplitude, which can contribute to TBC failure. Although the constraints in real TBC systems due to the ceramic layer and the TGO may change the diffusion kinetics, these processes would be important in inducing instability related TBC failures. Tailoring the BC materials to maximize resistance to diffusion can potentially minimize BC deformation and prolong the life of the TBC systems.

5 CONCLUSION

In the present work, isothermal experiments are carried out on nickel aluminide and platinum aluminide BC-superalloy systems in vacuum. The results show that rumpling can occur under isothermal conditions in absence of a significant oxide layer. The material concentration gradients in the BC cross-section did not show a strong correlation with the rumples. For nickel aluminide BC, the grain structure did not influence the rumpling behavior at high testing temperatures. As the isothermal ex-

posure temperature decreased, the BC grain boundaries increasingly influenced the rumpling behavior. For platinum aluminide BC, the rumples were correlated with the BC grains at the highest temperature of testing. Rumpling wavelength and amplitude were relatively insensitive to initial BC surface fluctuations in both material systems. Further, significant initial flaws are not needed for rumpling to occur. It is concluded that in absence of significant oxide layer, the driving force for rumpling formation is likely to be the thermal mismatch stress in the BC. Possible kinetics that governs the rumpling process in the present study includes a combination of diffusive processes such as surface, bulk and grain-boundary diffusion. These findings have strong implications in the TBC reliability study, since the diffusive processes in the BC driven by the BC stresses can potentially play a significant role in the TBC failure.

Acknowledgement

The work is supported by a Critical Research Initiative program at the University of Illinois at Urbana-Champaign (UIUC). One of the authors (R.P.) would like to thank the Fellowships Office at UIUC for their support through the Dissertation Completion Fellowship. Thanks go to Dr. Ram Darolia of General Electric for providing the superalloys, and to Paul Lawton, Stacy Fang, and Anthony Collucci of Chromally, NY, USA for coating the superalloys with the bond coat. We are thankful to Dr. Nancy Fennegan at UIUC for the AES work. The SEM, XRD, AES and profilometry was carried out in the Center for Microanalysis of Materials, Frederick Seitz Materials Research Laboratory, UIUC, which is partially supported by the U.S. Department of Energy under grant DEFG02-91-ER45439. The authors would like to acknowledge helpful discussions with Prof. David Cahill, Dr. Rick Haasch and Dr. Ming Liu at UIUC.

References

Ali, M. S., Song, S., & Xiao, P. 2002. Degradation of thermal barrier coatings due to thermal cycling up to 1150 °C. *J. Mater. Sci.*, 37, 2097–2102.

Ambrico, J. M., Begley, M., & Jordan, E. H. 2001. Stress and shape evolution in oxide films on elastic-plastic substrates due to thermal cycling and film growth. *Acta Mater.*, 49, 1577–1588.

Balint, D. S. & Hutchinson, J. W. 2003. Undulation instability of a compressed elastic film on a nonlinear creeping substrate. *Acta Mater.*, 51, 3965–3983.

Bartlett, A. H. & Maschio, R. D. 1995. Failure mechanisms of a zirconia-8% yttria thermal barrier coatings. *J. Am. Ceram. Soc.*, 78, 1018–1024.

Bartsch, M., Baufeld, B., & Fuller, E. R. J. 2003. Elucidating thermo-mechanical spallation of thermal barrier coating-systems using controlled indentation flaws. *Ceram. Eng. Sci. Proc.* to be published.

Bartsch, M., Marci, G., Mull, K., & Sick, C. 2001. Damage evolution in EB-PVD thermal barrier coatings for turbine blades in aircraft engines under close to reality testing conditions. *Int. J. Mat. Prod. Technol.*, 16, 248–257.

Baufeld, B. & Barstch, M. Effects of controlled thermal gradients in thermal mechanical fatigue. In Portella, P. D., Sehitoglu, H., & Hatanaka, K., ed., *Fifth International Conference on Low Cycle Fatigue, Berlin, Germany*. Federation of European Materials Societies, Sept 2003. to be published.

Baufeld, B., Tzimas, E., Mullejans, H., Peteves, S., Bressers, J., & Stamm, W. 2001. Thermal-mechanical fatigue of MAR-m 509 with a thermal barrier coating. *Mat. Sci. Engng.*, A315, 231–239.

Bose, S. & Demasi-Marcin, J. 1997. Thermal barrier coating experience in gas turbine engines at pratt and whitney. *J. Therm. Spray Technol.*, 6, 99–103.

Bouhanek, K., Adesanya, O. A., Stott, F. H., Skeldon, P., Lees, D. G., & Wood, G. C. 2000. Isothermal and thermal cyclic oxidation behavior of thermal barrier coatings: Pt aluminide bond coat. *Mat. High Temp.*, 2, 185–196.

Busso, E. P., Lin, J., Sakurai, S., & Nakayama, M. 2001. A mechanistic study of oxidation-induced degradation in a plasma-sprayed thermal barrier coating system: Part I: Model formulation. *Acta Mater.*, 49, 1515–1528.

Busso, E. P. & McClintock, F. A. 1993. Thermal fatigue degradation of an overlay coating. *Mater. Sci. Engng.*, A161, 165–179.

Chen, M. W., Ott, R. T., Hufnagel, T. C., Wright, P. K., & Hemker, K. J. 2003. Microstructural evolution of platinum modified nickel aluminide bond coat during thermal cycling. *Surf. Coat. Technol.*, 163-164, 25–30.

Clarke, D. R. & Shillington, E. A. G. 1999. Spalling failure of a thermal barrier coating associated with aluminum depletion in the bond-coat. *Acta Mater.*, 47, 1297–1305.

Deb, P., Boone, D. H., & Manley, T. F. I. 1987. Surface instability of platinum modified aluminized coatings during 1100 °C cyclic testing. *J. Vac. Sci. Technol.*, 5, 3366–3372.

Evans, A. G., Mumm, D. R., Hutchinson, J. W., Meier, G. H., & Pettit, F. S. 2001. Mechanisms controlling the durability of thermal barrier coatings. *Prog. Mat. Sci.*, 46, 505–553.

Finnie, K. R., Haasch, R., & Nuzzo, R. G. 2000. Formation and patterning of self-assembled monolayers driven from long-chain organosilicon amphiphiles and their use as templates in materials microfabrication. *Langmuir*, 16, 6968–6976.

Goward, G. W. 1998. Progress in coatings for gas turbine airfoils. *Surf. Coat. Technol.*, 108-109, 73–79.

He, M. Y., Evans, A. G., & Hutchinson, J. W. 2000. The ratcheting of compressed thermally grown thin films on ductile substrates. *Acta Mater.*, 48, 2593–2601.

Holmes, J. W. & McClintock, F. A. 1990. The chemical and mechanical processes of thermal fatigue degradation of an aluminide coating. *Metall. Trans.*, 21A, 1209–1222.

Ibegazene-Ouali, F., Mervel, R., Rio, C., & Renollet, Y. 2000. Microstructural evolution and degradation modes in cyclic and isothermal oxidation of an EB-PVD thermal barrier coating. *Mat. High Temp.*, 17, 205–218.

Karlsson, A. M. & Evans, A. G. 2001. A numerical model for the cyclic instability of thermally grown oxides in thermal barrier coatings. *Acta Mater.*, 49, 1793–1804.

Kim, G. M., Yanar, N. M., Hewitt, E. N., Pettit, F. S., & Meier, G. H. 2002. The effect of the type of thermal exposure on the durability of thermal barrier coatings. *Scripta Mater.*, 46, 489–495.

McDonald, G. & Hendricks, R. C. 1980. Effect of thermal cycling on ZrO_2-Y_2O_3 thermal barrier coatings. *Thin Solid Films*, 73, 491–496.

Meier, S. M. & Gupta, D. K. 1994. The evolution of thermal barrier coatings in gas turbine engine applications. *J. Eng. Gas Turbine Power*, 116, 250–257.

Miller, R. A. 1987. Current status of thermal barrier coatings-an overview. *Surf. Coat. Technol.*, 30, 1–11.

Miller, R. A. & Lowell, C. E. 1982. Failure mechanisms of thermal barrier coatings exposed to elevated temperatures. *Thin Solid Films*, 95, 265–273.

Mullins, W. W. *Solid Surface Morphologies Governed by Capillary.* American Society for Metals, Metals Park, OH, USA, 1963.

Mumm, D. R., Evans, A. G., & Spitsberg, I. T. 2001. Characterization of a cyclic displacement instability for a thermally grown oxide in a thermal barrier system. *Acta Mater.*, 49, 2329–2340.

Padture, N. P., Gell, M., & Jordan, E. H. 2002. Thermal barrier coatings for gas-turbine engine applications. *Science*, 296, 280–284.

Panat, R. P. & Hsia, K. J. 2003a. Experimental investigation of the bond coat rumpling instability under isothermal and cyclic thermal histories in thermal barrier systems. *Proc. Roy. Soc. London, Ser. A.* in press.

Panat, R. P. & Hsia, K. J. 2003b. On the evolution of stressed sinusoidal surfaces of films via volume and surface diffusion. *J. Appl. Phys.* submitted.

Panat, R. P., Zhang, S., & Hsia, K. J. 2003. Bond coat surface rumpling in thermal barrier coatings. *Acta Mater.*, 51, 239–249.

Pennefather, R. C. & Boone, D. H. 1995. Mechanical degradation of coating system in high-temperature cyclic oxidation. *Surf. Coat. Technol.*, 76-77, 47–52.

Ruud, J. A., Bartz, A., Borom, M. P., & Johnson, C. A. 2001. Strength degradation and failure mechanisms of EB-PVD thermal barrier coatings. *J. Am. Ceram. Soc.*, 84, 1545–1552.

Saif, M. T. A., Zhang, S., Haque, A., & Hsia, K. J. 2002. Effect of the native Al_2O_3 on the elastic response of nanoscale Al films. *Acta Mater.*, 50 (11), 2779–2786.

Schulz, U., Leyens, C., Fritscher, K. andPeters, M., Saruhan-Brings, B., Lavigne, O., Dorvaux, J., Poulain, Mevrel, R., & Calez, M. 2003. Some recent trends in research and technology of advanced thermal barrier coatings. *Aero. Sci. Technol.*, 7, 73–80.

Schulz, U., Menzebach, M., Leyens, C., & Yang, Y. Q. 2001. Influence of substrate material on oxidation behavior and cyclic lifetime of EB-PVD TBC systems. *Surf. Coat. Technol.*, 146-147, 117–123.

Sheffler, K. D. & Gupta, D. K. 1988. Current status and future trends in turbine applications of thermal barrier coatings. *J. Eng. Gas Turbine Power*, 110, 605–609.

Shewmon, P. G. *Diffusion in Solids.* Minerals, Metals & Materials Society, 2nd edition, 1989.

Stiger, M. J., Yanar, N. M., Topping, M. G., Pettit, F. S., & Meier, G. H. 1999. Thermal barrier coatings for the 21st century. *Z. Metallkd.*, 90(12), 1069–1078.

Strangman, T. E. 1985. Thermal barrier coatings for turbine airfoils. *Thin Solid Films*, 127, 93–106.

Strohmeier, B. 1990. An ESCA method for determining the oxide thickness on aluminum alloys. *Surf. Interf. Anal.*, 15, 51–56.

Suo, Z. 1995. Wrinkling of the oxide scale on an aluminium-containing alloy at high temperatures. *J. Mech. Phys. Solids*, 43, 829–846.

Suo, Z., Kubair, D., Evans, A. G., Clarke, D. R., & Tolpygo, V. 2003. Stresses induced in alloys by selective oxidation. *Acta Mater.*, 51, 959–974.

Thouless, M. D. 1993. Effect of surface diffusion on the creep of thin films and sintered arrays of particles. *Acta Metall. Mater.*, 41, 1057–1064.

Tolpygo, V. K. & Clarke, D. R. 2000. Surface rumpling of a (Ni,Pt)Al bond coat induced by cyclic oxidation. *Acta Mater.*, 48, 3283–3293.

Tolpygo, V. K. & Clarke, D. R. Damage induced by thermal cycling of thermal barrier coatings. In Dahotre, N. B., Hampikian, J. M., & Morral, J. E., ed., *Elevated Temperature Coatings: Science & Technology IV*, pp. 94. TMS, 2001.

Tolpygo, V. K., Clarke, D. R., & Murphy, K. S. 2001. Oxidation induced failure of EB-PVD thermal barrier coatings. *Surf. Coat. Technol.*, 146-147, 124–134.

Vaidyanathan, K., Gell, M., & Jordan, E. 2000. Mechanisms of spallation of electron beam physical vapor deposited thermal barrier coatings with and without platinum aluminide bond coat ridges. *Surf. Coat. Technol.*, 133-134, 28–34.

Walston, W. S., O'Hara, K. S., Ross, E. W., Pollock, T. M., & Murphy, W. H. René N6: Third generation single crystal superalloy. In Kissinger, R. D., Deye, D. J., Anton, D. L., Cetel, A. D., Nathal, M. V., Pollock, T. M., & Woodford, D. A., ed., *Proc. Superalloys Symp.*, pp. 27–33. The Minerals, Metals & Materials Society (TMS), 1996.

Watanabe, M., Mumm, D. R., Chiras, S., & Evans, A. G. 2002. Measurement of the residual stress in a Pt-aluminide bond coat. *Scripta Mater.*, 46, 67–70.

Wright, P. K. 1998. Influence of cyclic strain on life of a PVD TBC. *Mater. Sci. Engng.*, A245, 191–200.

Wright, P. K. & Evans, A. G. 1999. Mechanisms governing the performance of thermal barrier coatings. *Curr. Op. Sol. St. & Mat. Sci.*, 4, 255–265.

Wu, B. C., Chang, E., Chang, S. F., & Chao, C. H. 1989. Thermal cyclic response of yttria-stabilized zirconia/CoNiCrAlY thermal barrier coatings. *Thin Solid Films*, 172, 185–196.

Zhang, Y. H., Withers, P. J., Fox, M. D., & Knowles, D. M. 1999. Damage mechanisms of coated systems under thermomechanical fatigue. *Mat. Sci. Technol.*, 15, 1031–1036.

Table 1: Summary of experiments

Testing condition	Initial surface	Nickel aluminide BC	Platinum aluminide BC
1200 °C 50 hours	polished	Surface rumpled with little or no correlation with BC grain structure	Surface rumpled with fluctuations correlated with BC grain structure
1200 °C 25 hours	as deposited	Surface rumpled with little or no correlation with BC grain structure	no observations due to non-uniform oxide formation
1175 °C 50 hours	partially polished	Surface rumpled with some correlation to BC grain structure	– same as above –
1150 °C 25 hours	polished	Surface fluctuations correlated with BC grain structure	– same as above –

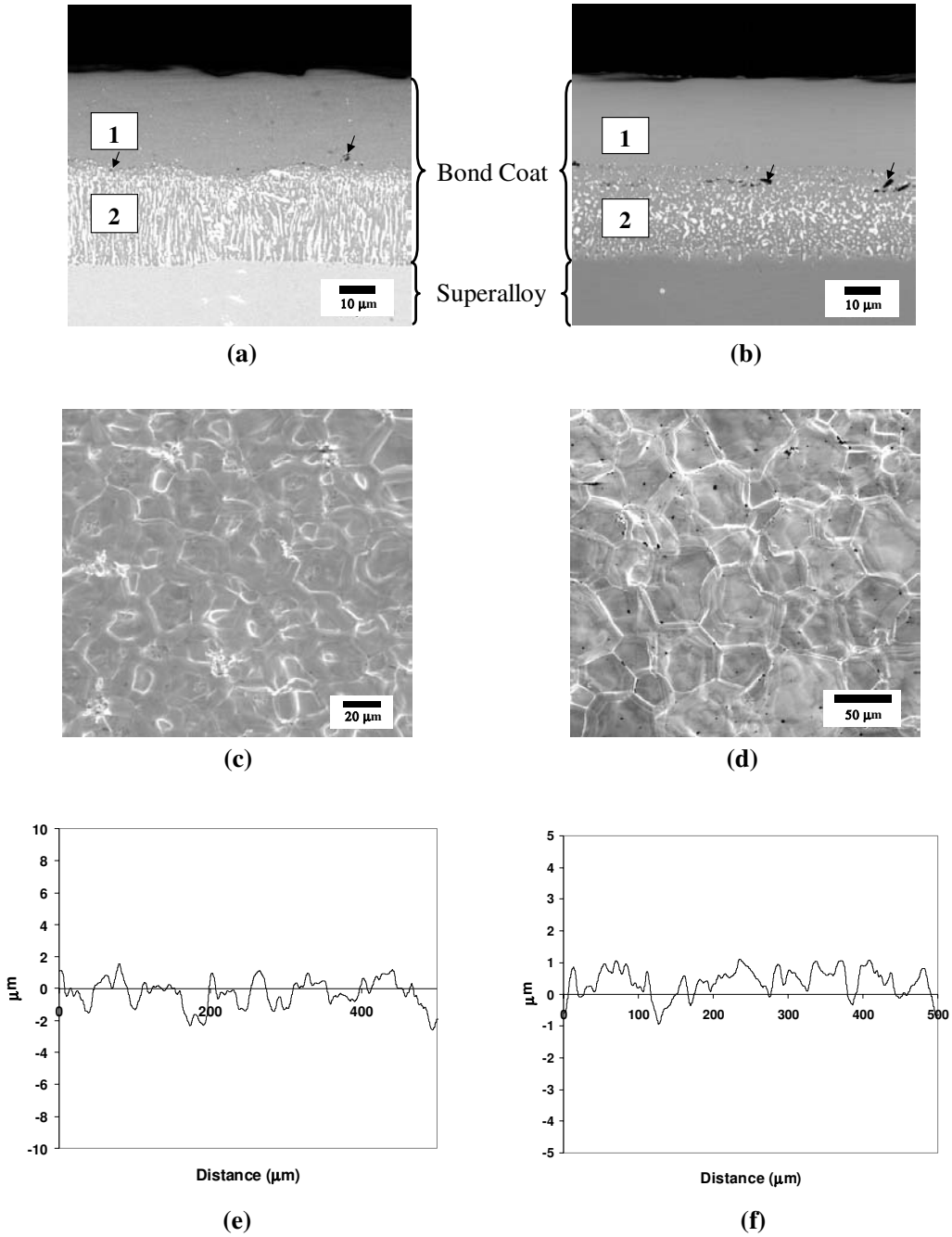

Figure 1: Cross-sectional SEM micrographs (with backscatter electrons) of (a) Nickel aluminide BC and (b) Platinum aluminide BC. Both BCs show outer zone, '1' and interdiffusion zone, '2'. Black arrows show alumina inclusions regularly placed between the two regions. (c,d) Top views of the nickel aluminide and the platinum aluminide BC, respectively. Ridges along the grain boundaries are clearly visible. (e,f) Profilometer scans of the nickel aluminide and platinum aluminide BC surfaces, respectively.

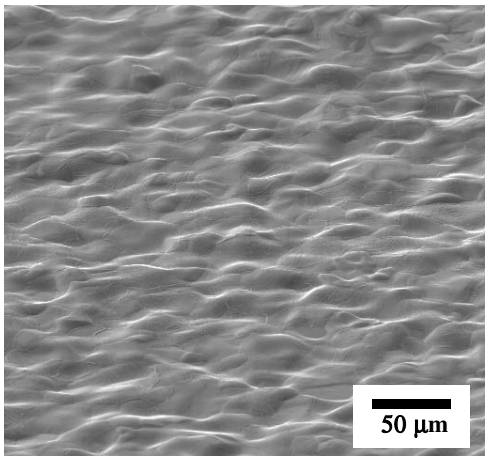

(a)

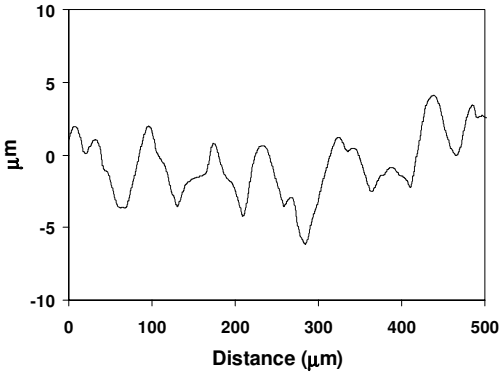

(b)

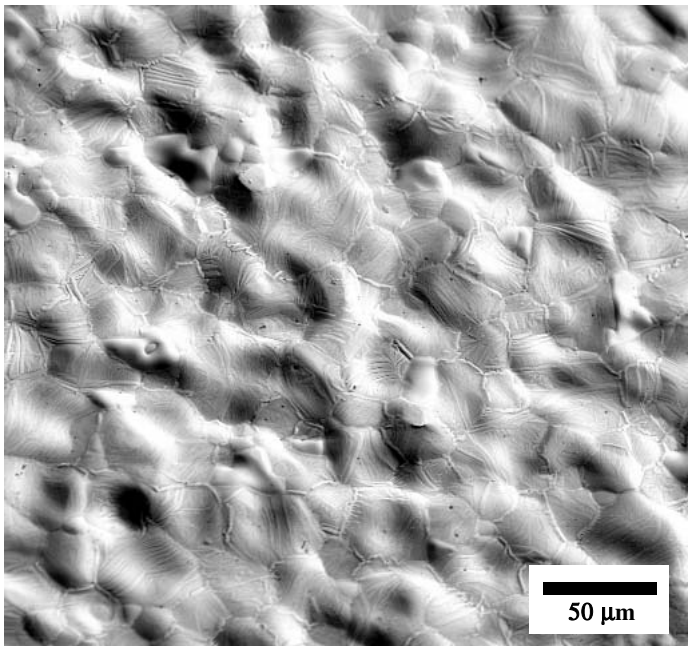

(c)

Figure 2: Nickel aluminide BC after 25 hour isothermal exposure at 1200 °C in vacuum. (a) SEM micrograph showing BC surface rumpling, (b) corresponding profilometer scan. The micrograph is taken at a tilt of 30° to the BC top surface. (c) Top view of the same surface showing grains and rumpling. The BC grains have little correlation with the rumple formation.

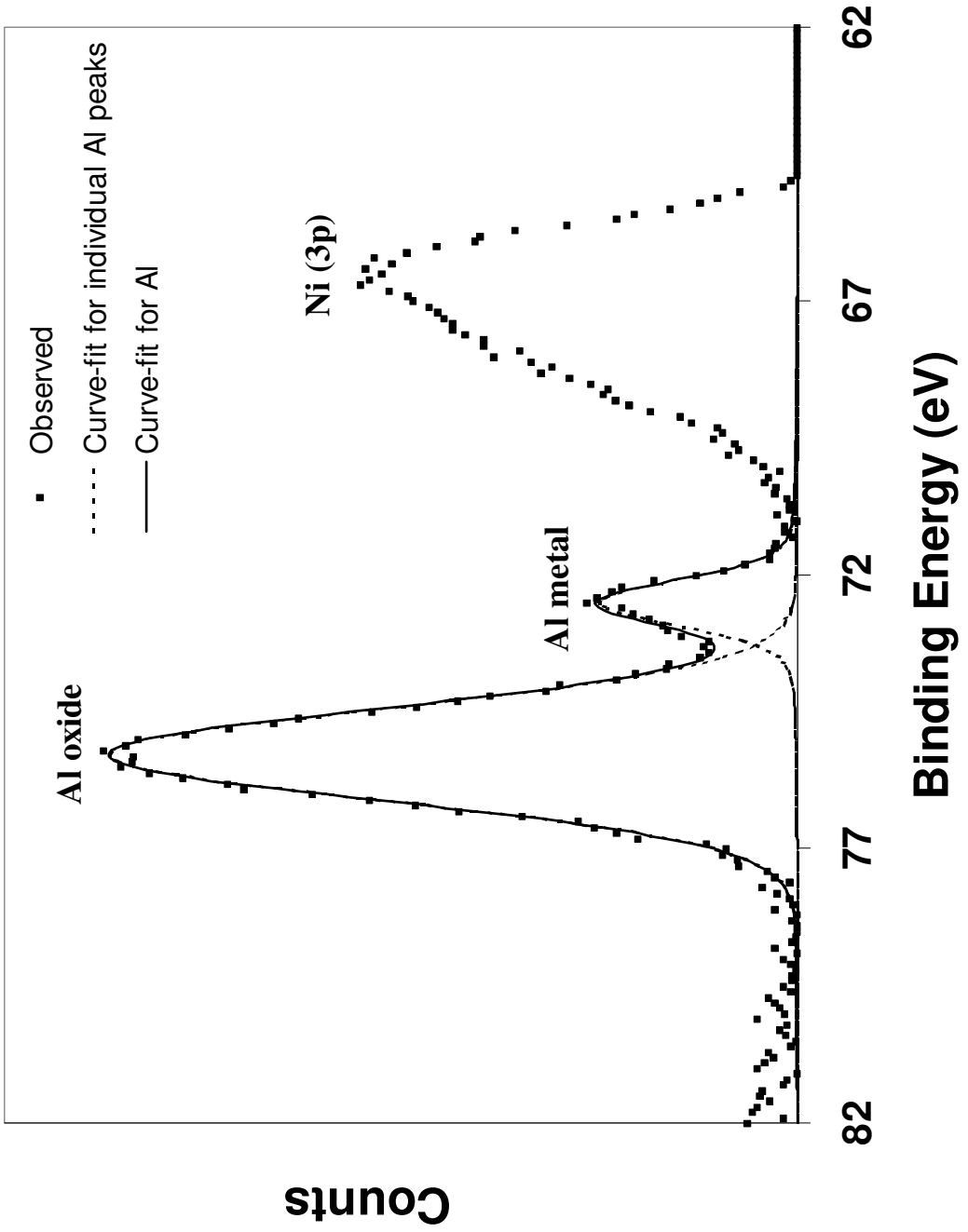

Figure 3: XPS spectrum of the BC surface showing Al 2p peak envelop. The fitted curves for the individual peaks give the areas under the Al 2p peaks representing Al metal and Al oxide. The relative areas under the peaks representing Al metal and Al oxide can be used to estimate the Al oxide layer thickness. An additional peak due to Ni 3p is also seen.

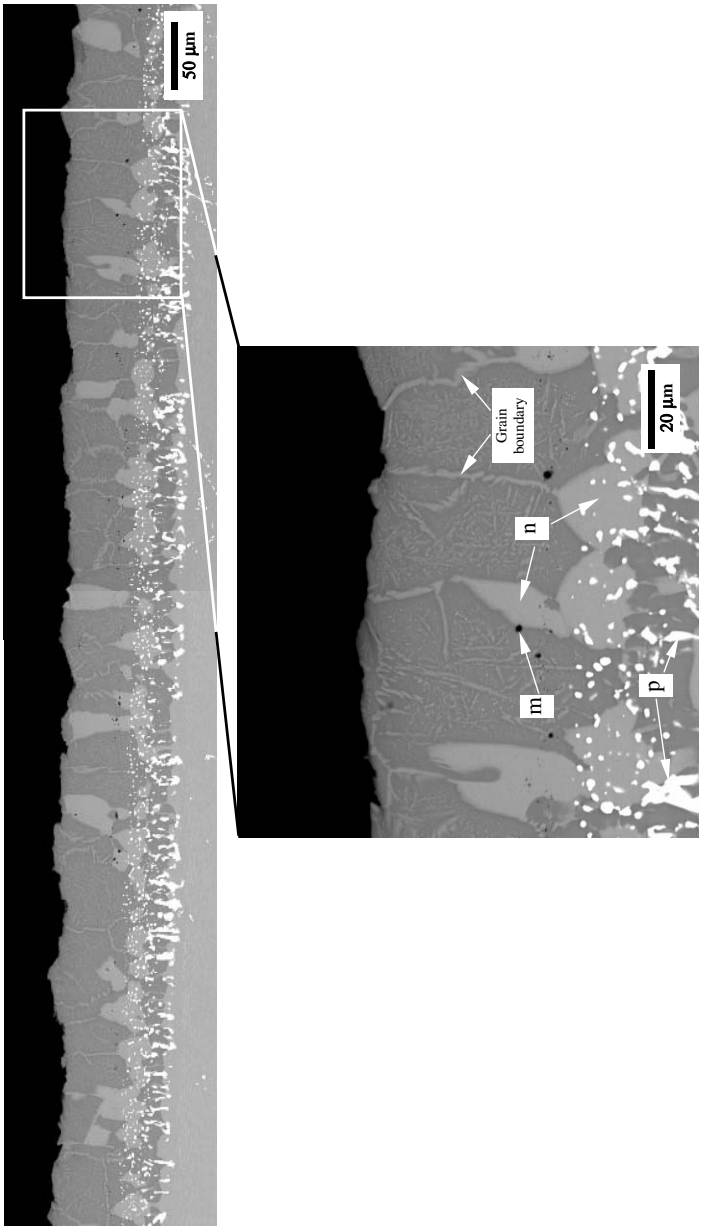

Figure 4: A representative SEM micrograph (with backscatter electrons) of the nickel aluminide BC cross section showing the microstructure after 25 hour isothermal exposure at 1200 °C. The grain boundaries can be seen as brighter regions in the cross section as indicated in the micrograph with higher magnification. Large bright regions indicated by "n" are seen to have developed along the grain boundaries. Alumina inclusions denoted by "m" are seen as the dark regions at the boundary of the outer and the inner region of the BC. These alumina inclusions were present before the isothermal exposure (Fig. 1a). Regions "p" represent precipitates rich in W, Mo and Ta, also present before thermal cycling (Fig. 1a).

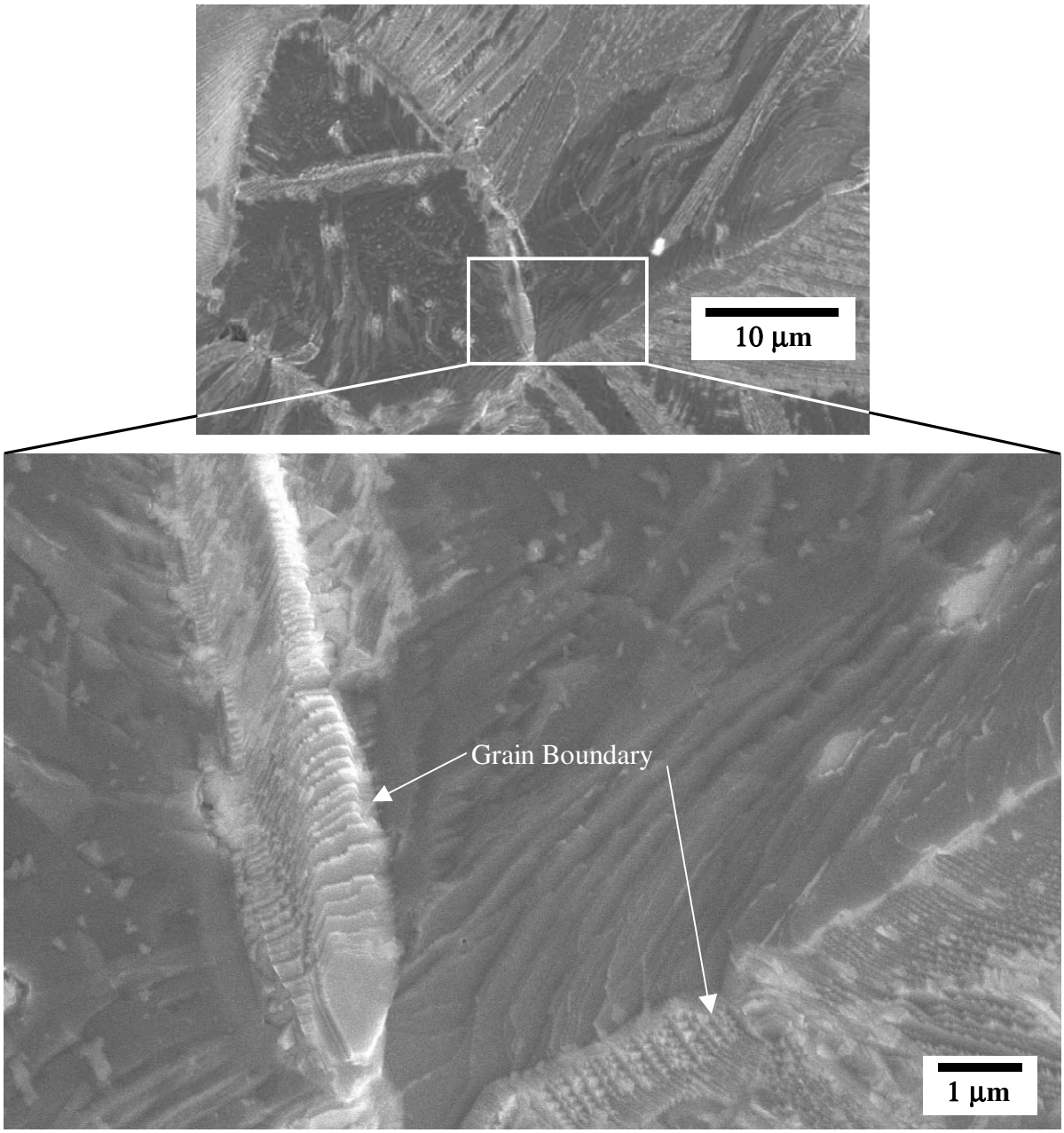

Figure 5: SEM micrographs showing faceting of the grain boundaries and grain surfaces of nickel aluminide BC surface after 25 hour isothermal exposure at 1200 °C in vacuum.

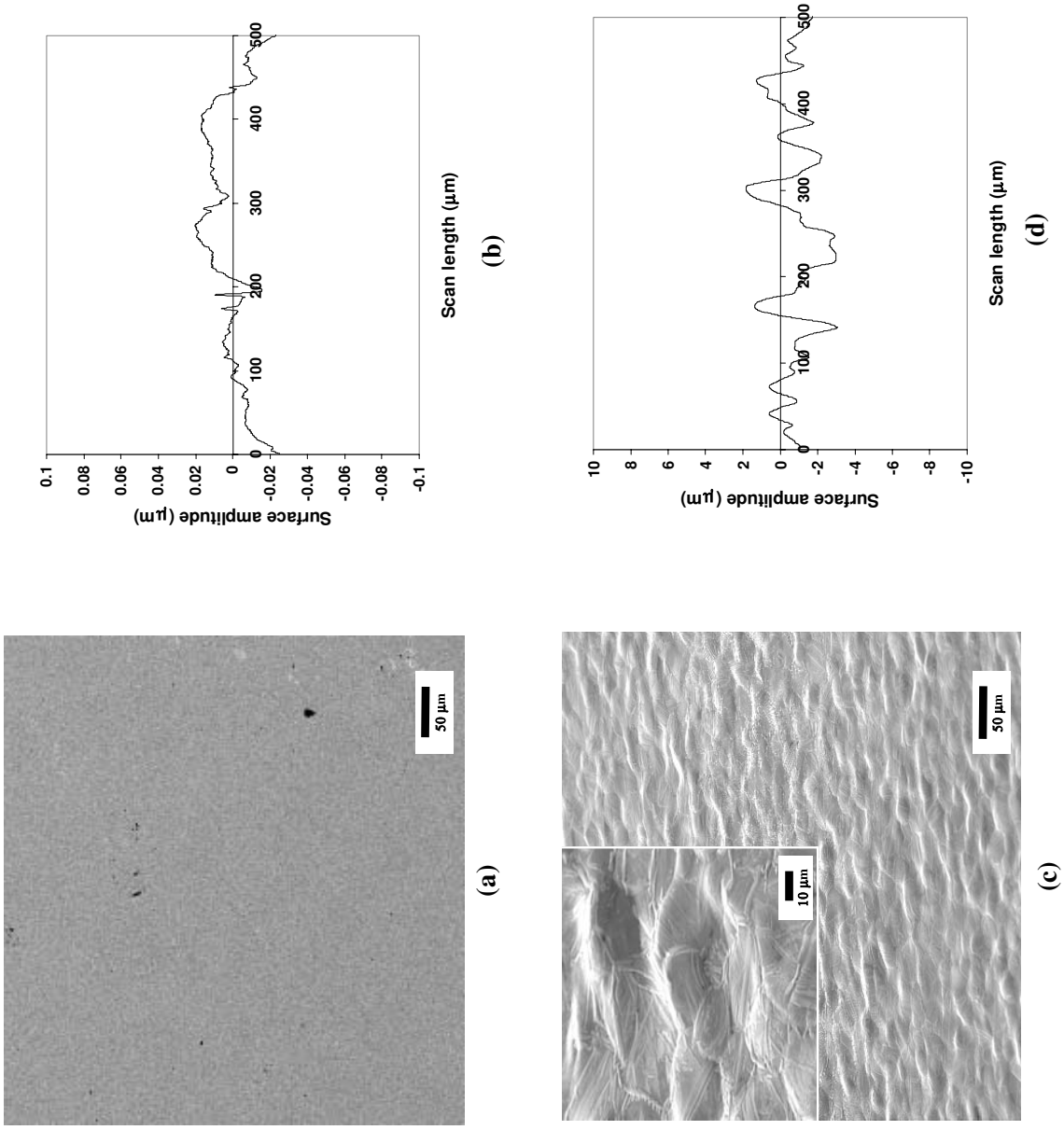

Figure 6: (a,b) SEM micrograph of the initial surface of a nickel aluminide BC and the corresponding profilometer scan; (c,d) SEM micrograph showing the rumpling of the same BC surface after 50 hours at 1200 °C in vacuum. (d) The profilometer scan of the surface shown in (c). The micrographs are taken at a tilt of 30° to the BC top surface.

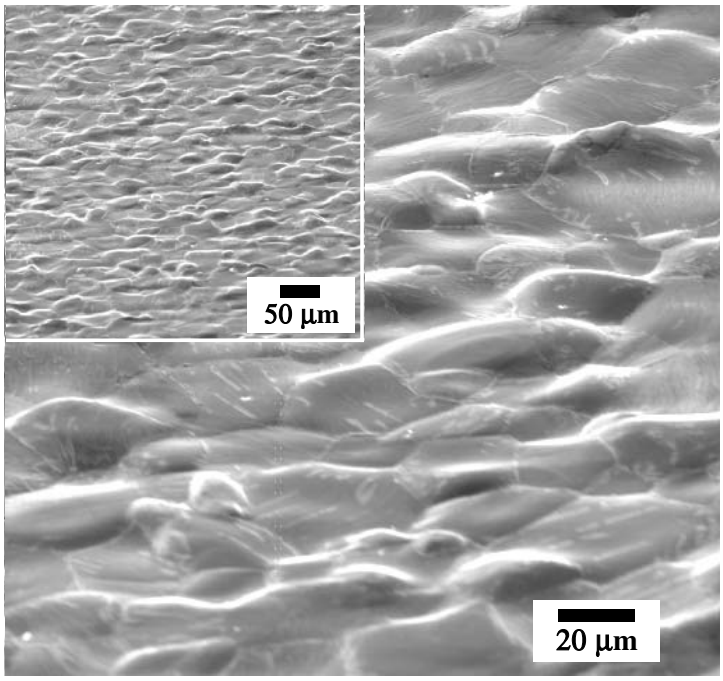

(a)

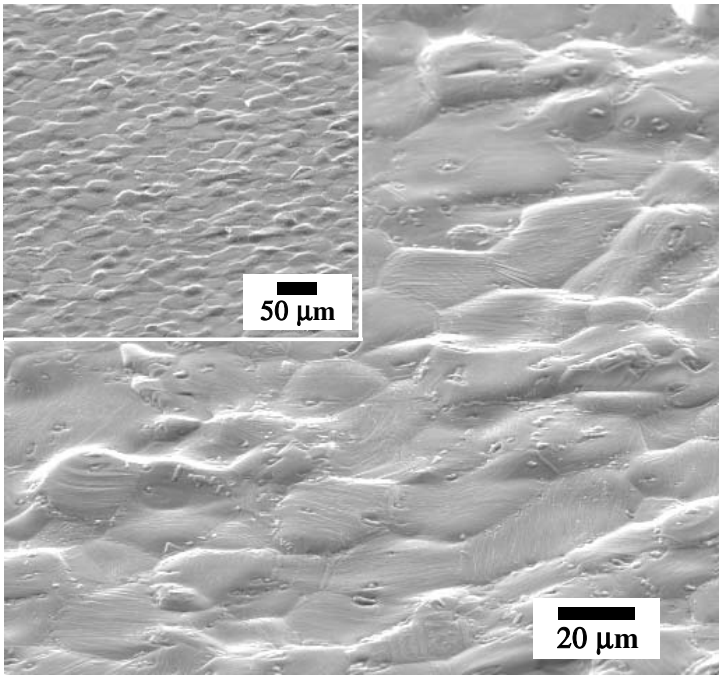

(b)

Figure 7: SEM micrograph showing the nickel aluminide BC (a) after 50 hour exposure at 1175 °C in vacuum, and (b) after 25 hour exposure to 1150 °C in vacuum. The micrographs are taken at a tilt of 30° (a) and 42° (b) to the BC top surface.

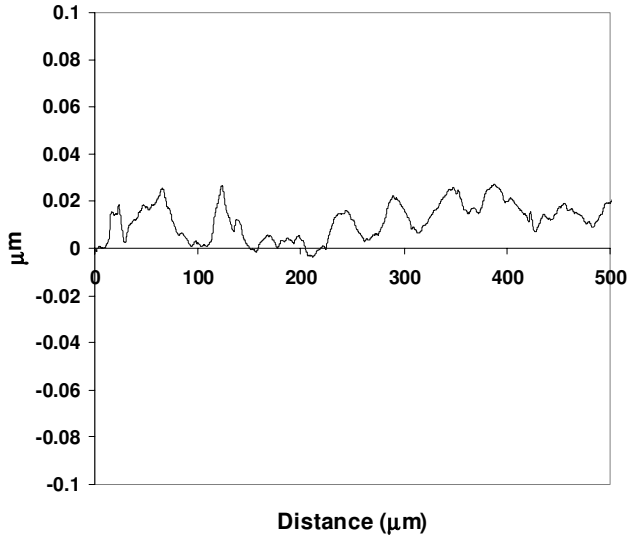

(a)

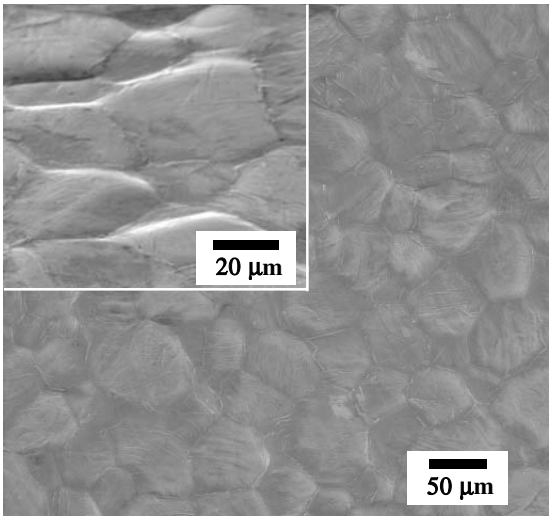

(b)

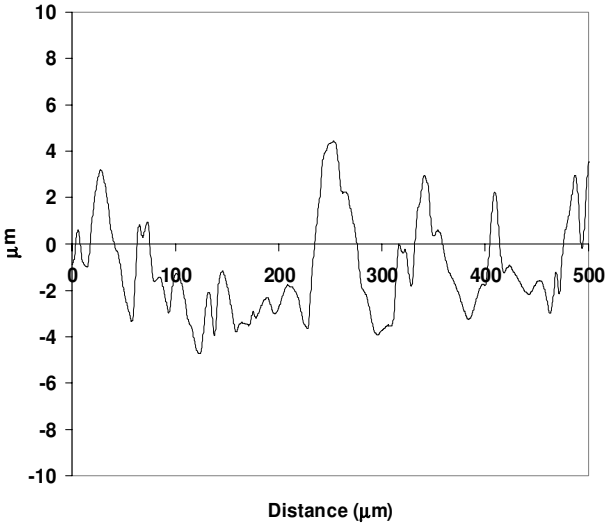

(c)

Figure 8: Platinum aluminide BC (a) profilometer scan before thermal treatment, (b) SEM micrograph after 50 hour exposure at 1200 °C in vacuum, and (c) The profilometer scan of the surface shown in (b). The high magnification inset in (b) is taken at a tilt of 30° to the BC top surface.

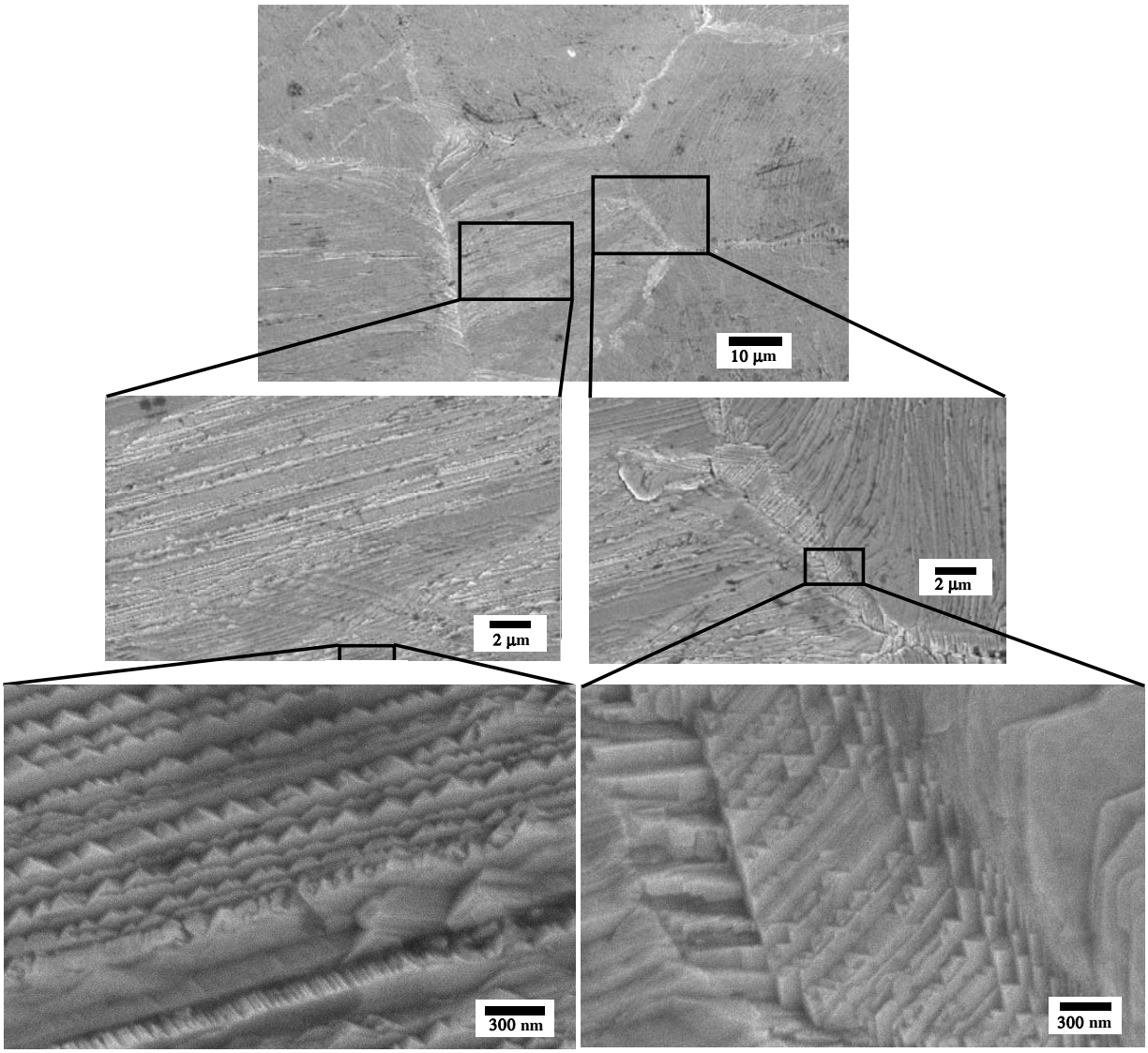

Figure 9: High magnification SEM micrographs of the rumpled platinum aluminide BC shown in Fig. 8b. Extensive facets developed over the grain surface and a "depressed" grain boundary (also showing facets) can be seen.

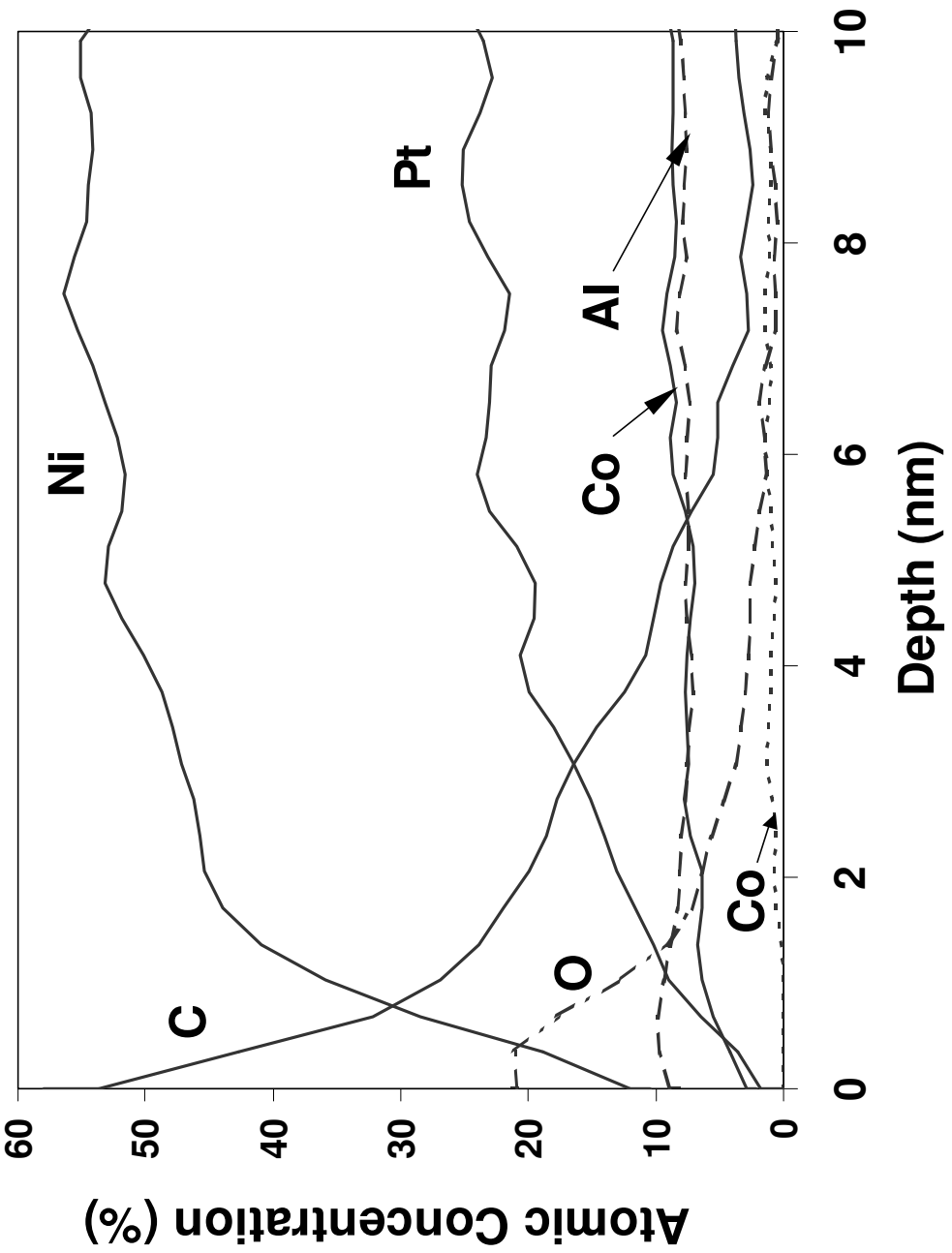

Figure 10: AES spectrum of the platinum aluminide BC surface shown in Fig. 8b as a function of sputter depth.

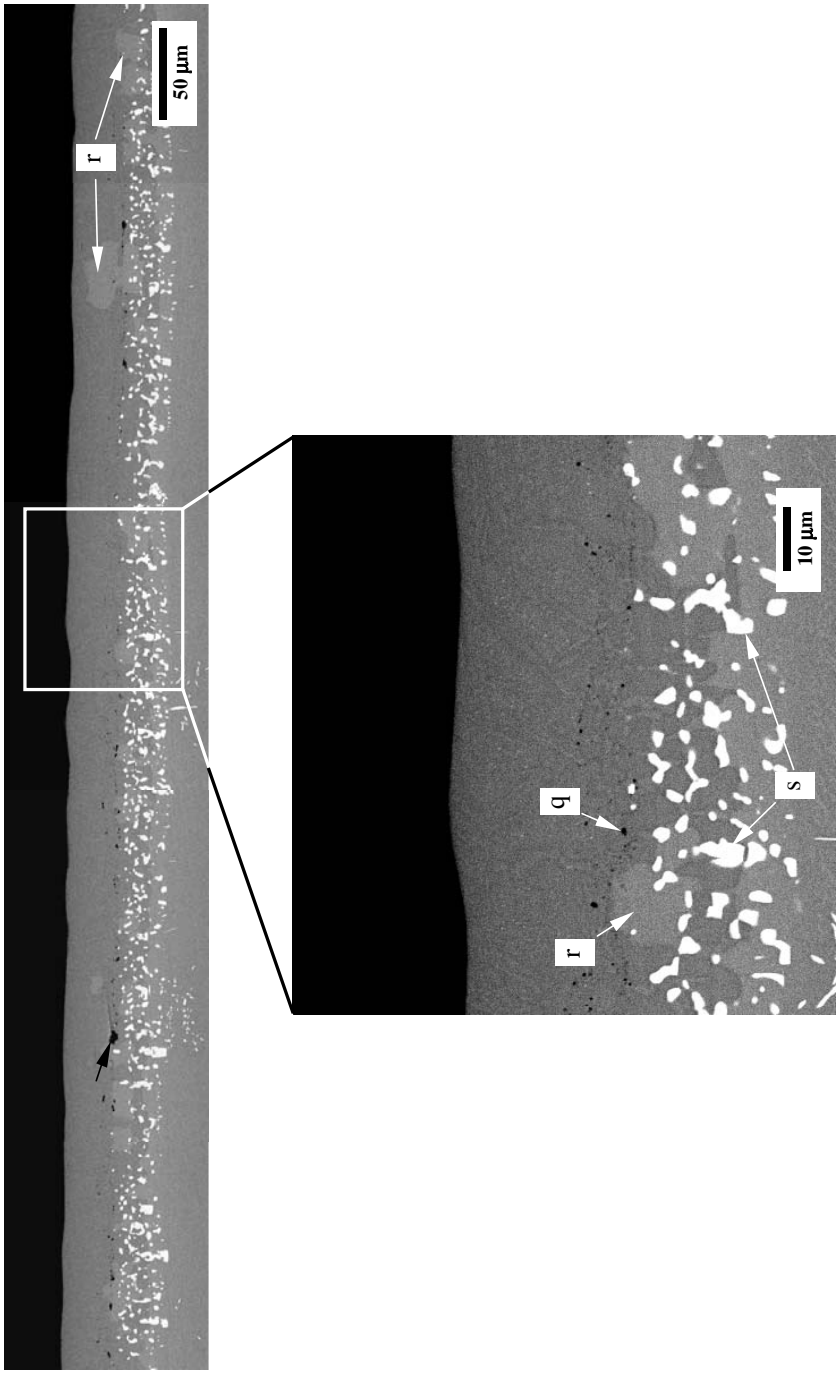

Figure 11: A representative SEM micrograph (with backscatter electrons) of the platinum aluminide BC cross section showing the microstructure after 50 hour isothermal exposure at 1200 °C. Large bright regions (denoted by "r") and alumina inclusions (denoted by "q") are seen to have developed at the boundary between the outer and the inner regions. The alumina inclusions were present before the isothermal exposure (Fig. 1a). An isolated void is shown by a black arrow. Regions "s" represent precipitates rich in W, Mo and Ta that were also present before thermal cycling (Fig. 1a).

List of Recent TAM Reports

No.	Authors	Title	Date
953	Riahi, D. N., and A. T. Hsui	A theoretical investigation of high Rayleigh number convection in a nonuniform gravitational field—*International Journal of Pure and Applied Mathematics*, in press (2003)	Aug. 2000
954	Riahi, D. N.	Effects of centrifugal and Coriolis forces on a hydromagnetic chimney convection in a mushy layer—*Journal of Crystal Growth* **226**, 393–405 (2001)	Aug. 2000
955	Fried, E.	An elementary molecular-statistical basis for the Mooney and Rivlin–Saunders theories of rubber-elasticity—*Journal of the Mechanics and Physics of Solids* **50**, 571–582 (2002)	Sept. 2000
956	Phillips, W. R. C.	On an instability to Langmuir circulations and the role of Prandtl and Richardson numbers—*Journal of Fluid Mechanics* **442**, 335–358 (2001)	Sept. 2000
957	Chaïeb, S., and J. Sutin	Growth of myelin figures made of water soluble surfactant—Proceedings of the 1st Annual International IEEE–EMBS Conference on Microtechnologies in Medicine and Biology (October 2000, Lyon, France), 345–348	Oct. 2000
958	Christensen, K. T., and R. J. Adrian	Statistical evidence of hairpin vortex packets in wall turbulence—*Journal of Fluid Mechanics* **431**, 433–443 (2001)	Oct. 2000
959	Kuznetsov, I. R., and D. S. Stewart	Modeling the thermal expansion boundary layer during the combustion of energetic materials—*Combustion and Flame*, in press (2001)	Oct. 2000
960	Zhang, S., K. J. Hsia, and A. J. Pearlstein	Potential flow model of cavitation-induced interfacial fracture in a confined ductile layer—*Journal of the Mechanics and Physics of Solids*, **50**, 549–569 (2002)	Nov. 2000
961	Sharp, K. V., R. J. Adrian, J. G. Santiago, and J. I. Molho	Liquid flows in microchannels—Chapter 6 of *CRC Handbook of MEMS* (M. Gad-el-Hak, ed.) (2001)	Nov. 2000
962	Harris, J. G.	Rayleigh wave propagation in curved waveguides—*Wave Motion* **36**, 425–441 (2002)	Jan. 2001
963	Dong, F., A. T. Hsui, and D. N. Riahi	A stability analysis and some numerical computations for thermal convection with a variable buoyancy factor—*Journal of Theoretical and Applied Mechanics* **2**, 19–46 (2002)	Jan. 2001
964	Phillips, W. R. C.	Langmuir circulations beneath growing or decaying surface waves—*Journal of Fluid Mechanics* (submitted)	Jan. 2001
965	Bdzil, J. B., D. S. Stewart, and T. L. Jackson	Program burn algorithms based on detonation shock dynamics—*Journal of Computational Physics* (submitted)	Jan. 2001
966	Bagchi, P., and S. Balachandar	Linearly varying ambient flow past a sphere at finite Reynolds number: Part 2—Equation of motion—*Journal of Fluid Mechanics* **481**, 105–148 (2003) (with change in title)	Feb. 2001
967	Cermelli, P., and E. Fried	The evolution equation for a disclination in a nematic fluid—*Proceedings of the Royal Society A* **458**, 1–20 (2002)	Apr. 2001
968	Riahi, D. N.	Effects of rotation on convection in a porous layer during alloy solidification—Chapter 12 in *Transport Phenomena in Porous Media* (D. B. Ingham and I. Pop, eds.), 316–340 (2002)	Apr. 2001
969	Damljanovic, V., and R. L. Weaver	Elastic waves in cylindrical waveguides of arbitrary cross section—*Journal of Sound and Vibration* (submitted)	May 2001
970	Gioia, G., and A. M. Cuitiño	Two-phase densification of cohesive granular aggregates—*Physical Review Letters* **88**, 204302 (2002) (in extended form and with added co-authors S. Zheng and T. Uribe)	May 2001
971	Subramanian, S. J., and P. Sofronis	Calculation of a constitutive potential for isostatic powder compaction—*International Journal of Mechanical Sciences* (submitted)	June 2001
972	Sofronis, P., and I. M. Robertson	Atomistic scale experimental observations and micromechanical/continuum models for the effect of hydrogen on the mechanical behavior of metals—*Philosophical Magazine* (submitted)	June 2001

List of Recent TAM Reports (cont'd)

No.	Authors	Title	Date
973	Pushkin, D. O., and H. Aref	Self-similarity theory of stationary coagulation—*Physics of Fluids* **14**, 694–703 (2002)	July 2001
974	Lian, L., and N. R. Sottos	Stress effects in ferroelectric thin films—*Journal of the Mechanics and Physics of Solids* (submitted)	Aug. 2001
975	Fried, E., and R. E. Todres	Prediction of disclinations in nematic elastomers—*Proceedings of the National Academy of Sciences* **98**, 14773–14777 (2001)	Aug. 2001
976	Fried, E., and V. A. Korchagin	Striping of nematic elastomers—*International Journal of Solids and Structures* **39**, 3451–3467 (2002)	Aug. 2001
977	Riahi, D. N.	On nonlinear convection in mushy layers: Part I. Oscillatory modes of convection—*Journal of Fluid Mechanics* **467**, 331–359 (2002)	Sept. 2001
978	Sofronis, P., I. M. Robertson, Y. Liang, D. F. Teter, and N. Aravas	Recent advances in the study of hydrogen embrittlement at the University of Illinois—Invited paper, Hydrogen–Corrosion Deformation Interactions (Sept. 16–21, 2001, Jackson Lake Lodge, Wyo.)	Sept. 2001
979	Fried, E., M. E. Gurtin, and K. Hutter	A void-based description of compaction and segregation in flowing granular materials—*Continuum Mechanics and Thermodynamics*, in press (2003)	Sept. 2001
980	Adrian, R. J., S. Balachandar, and Z.-C. Liu	Spanwise growth of vortex structure in wall turbulence—*Korean Society of Mechanical Engineers International Journal* **15**, 1741–1749 (2001)	Sept. 2001
981	Adrian, R. J.	Information and the study of turbulence and complex flow—*Japanese Society of Mechanical Engineers Journal B*, in press (2002)	Oct. 2001
982	Adrian, R. J., and Z.-C. Liu	Observation of vortex packets in direct numerical simulation of fully turbulent channel flow—*Journal of Visualization*, in press (2002)	Oct. 2001
983	Fried, E., and R. E. Todres	Disclinated states in nematic elastomers—*Journal of the Mechanics and Physics of Solids* **50**, 2691–2716 (2002)	Oct. 2001
984	Stewart, D. S.	Towards the miniaturization of explosive technology—Proceedings of the 23rd International Conference on Shock Waves (2001)	Oct. 2001
985	Kasimov, A. R., and Stewart, D. S.	Spinning instability of gaseous detonations—*Journal of Fluid Mechanics* (submitted)	Oct. 2001
986	Brown, E. N., N. R. Sottos, and S. R. White	Fracture testing of a self-healing polymer composite—*Experimental Mechanics* (submitted)	Nov. 2001
987	Phillips, W. R. C.	Langmuir circulations—*Surface Waves* (J. C. R. Hunt and S. Sajjadi, eds.), in press (2002)	Nov. 2001
988	Gioia, G., and F. A. Bombardelli	Scaling and similarity in rough channel flows—*Physical Review Letters* **88**, 014501 (2002)	Nov. 2001
989	Riahi, D. N.	On stationary and oscillatory modes of flow instabilities in a rotating porous layer during alloy solidification—*Journal of Porous Media* **6**, 1–11 (2003)	Nov. 2001
990	Okhuysen, B. S., and D. N. Riahi	Effect of Coriolis force on instabilities of liquid and mushy regions during alloy solidification—*Physics of Fluids* (submitted)	Dec. 2001
991	Christensen, K. T., and R. J. Adrian	Measurement of instantaneous Eulerian acceleration fields by particle-image accelerometry: Method and accuracy—*Experimental Fluids* (submitted)	Dec. 2001
992	Liu, M., and K. J. Hsia	Interfacial cracks between piezoelectric and elastic materials under in-plane electric loading—*Journal of the Mechanics and Physics of Solids* **51**, 921–944 (2003)	Dec. 2001
993	Panat, R. P., S. Zhang, and K. J. Hsia	Bond coat surface rumpling in thermal barrier coatings—*Acta Materialia* **51**, 239–249 (2003)	Jan. 2002
994	Aref, H.	A transformation of the point vortex equations—*Physics of Fluids* **14**, 2395–2401 (2002)	Jan. 2002
995	Saif, M. T. A, S. Zhang, A. Haque, and K. J. Hsia	Effect of native Al_2O_3 on the elastic response of nanoscale aluminum films—*Acta Materialia* **50**, 2779–2786 (2002)	Jan. 2002

List of Recent TAM Reports (cont'd)

No.	*Authors*	*Title*	*Date*
996	Fried, E., and M. E. Gurtin	A nonequilibrium theory of epitaxial growth that accounts for surface stress and surface diffusion—*Journal of the Mechanics and Physics of Solids* **51**, 487–517 (2003)	Jan. 2002
997	Aref, H.	The development of chaotic advection—*Physics of Fluids* **14**, 1315–1325 (2002); see also *Virtual Journal of Nanoscale Science and Technology*, 11 March 2002	Jan. 2002
998	Christensen, K. T., and R. J. Adrian	The velocity and acceleration signatures of small-scale vortices in turbulent channel flow—*Journal of Turbulence*, in press (2002)	Jan. 2002
999	Riahi, D. N.	Flow instabilities in a horizontal dendrite layer rotating about an inclined axis—*Journal of Porous Media*, in press (2003)	Feb. 2002
1000	Kessler, M. R., and S. R. White	Cure kinetics of ring-opening metathesis polymerization of dicyclopentadiene—*Journal of Polymer Science A* **40**, 2373–2383 (2002)	Feb. 2002
1001	Dolbow, J. E., E. Fried, and A. Q. Shen	Point defects in nematic gels: The case for hedgehogs—*Proceedings of the National Academy of Sciences* (submitted)	Feb. 2002
1002	Riahi, D. N.	Nonlinear steady convection in rotating mushy layers—*Journal of Fluid Mechanics* **485**, 279–306 (2003)	Mar. 2002
1003	Carlson, D. E., E. Fried, and S. Sellers	The totality of soft-states in a neo-classical nematic elastomer—*Journal of Elasticity* **69**, 169–180 (2003) with revised title	Mar. 2002
1004	Fried, E., and R. E. Todres	Normal-stress differences and the detection of disclinations in nematic elastomers—*Journal of Polymer Science B: Polymer Physics* **40**, 2098–2106 (2002)	June 2002
1005	Fried, E., and B. C. Roy	Gravity-induced segregation of cohesionless granular mixtures—*Lecture Notes in Mechanics*, in press (2002)	July 2002
1006	Tomkins, C. D., and R. J. Adrian	Spanwise structure and scale growth in turbulent boundary layers—*Journal of Fluid Mechanics* (submitted)	Aug. 2002
1007	Riahi, D. N.	On nonlinear convection in mushy layers: Part 2. Mixed oscillatory and stationary modes of convection—*Journal of Fluid Mechanics* (submitted)	Sept. 2002
1008	Aref, H., P. K. Newton, M. A. Stremler, T. Tokieda, and D. L. Vainchtein	Vortex crystals—*Advances in Applied Mathematics* **39**, in press (2002)	Oct. 2002
1009	Bagchi, P., and S. Balachandar	Effect of turbulence on the drag and lift of a particle—*Physics of Fluids*, in press (2003)	Oct. 2002
1010	Zhang, S., R. Panat, and K. J. Hsia	Influence of surface morphology on the adhesive strength of aluminum/epoxy interfaces—*Journal of Adhesion Science and Technology* **17**, 1685–1711 (2003)	Oct. 2002
1011	Carlson, D. E., E. Fried, and D. A. Tortorelli	On internal constraints in continuum mechanics—*Journal of Elasticity* **70**, 101–109 (2003)	Oct. 2002
1012	Boyland, P. L., M. A. Stremler, and H. Aref	Topological fluid mechanics of point vortex motions—*Physica D* **175**, 69–95 (2002)	Oct. 2002
1013	Bhattacharjee, P., and D. N. Riahi	Computational studies of the effect of rotation on convection during protein crystallization—*Journal of Crystal Growth* (submitted)	Feb. 2003
1014	Brown, E. N., M. R. Kessler, N. R. Sottos, and S. R. White	*In situ* poly(urea-formaldehyde) microencapsulation of dicyclopentadiene—*Journal of Microencapsulation* (submitted)	Feb. 2003
1015	Brown, E. N., S. R. White, and N. R. Sottos	Microcapsule induced toughening in a self-healing polymer composite—*Journal of Materials Science* (submitted)	Feb. 2003
1016	Kuznetsov, I. R., and D. S. Stewart	Burning rate of energetic materials with thermal expansion—*Combustion and Flame* (submitted)	Mar. 2003
1017	Dolbow, J., E. Fried, and H. Ji	Chemically induced swelling of hydrogels—*Journal of the Mechanics and Physics of Solids*, in press (2003)	Mar. 2003

List of Recent TAM Reports (cont'd)

No.	*Authors*	*Title*	*Date*
1018	Costello, G. A.	Mechanics of wire rope—Mordica Lecture, Interwire 2003, Wire Association International, Atlanta, Georgia, May 12, 2003	Mar. 2003
1019	Wang, J., N. R. Sottos, and R. L. Weaver	Thin film adhesion measurement by laser induced stress waves—*Journal of the Mechanics and Physics of Solids* (submitted)	Apr. 2003
1020	Bhattacharjee, P., and D. N. Riahi	Effect of rotation on surface tension driven flow during protein crystallization—*Microgravity Science and Technology*, in press (2003)	Apr. 2003
1021	Fried, E.	The configurational and standard force balances are not always statements of a single law—*Proceedings of the Royal Society* (submitted)	Apr. 2003
1022	Panat, R. P., and K. J. Hsia	Experimental investigation of the bond coat rumpling instability under isothermal and cyclic thermal histories in thermal barrier systems—*Proceedings of the Royal Society of London A*, in press (2003)	May 2003
1023	Fried, E., and M. E. Gurtin	A unified treatment of evolving interfaces accounting for small deformations and atomic transport: grain-boundaries, phase transitions, epitaxy—*Advances in Applied Mechanics*, in press (2003)	May 2003
1024	Dong, F., D. N. Riahi, and A. T. Hsui	On similarity waves in compacting media—*Horizons in Physics*, in press (2003)	May 2003
1025	Liu, M., and K. J. Hsia	Locking of electric field induced non-180° domain switching and phase transition in ferroelectric materials upon cyclic electric fatigue—*Applied Physics Letters*, in press (2003)	May 2003
1026	Liu, M., K. J. Hsia, and M. Sardela Jr.	In situ X-ray diffraction study of electric field induced domain switching and phase transition in PZT-5H—*Journal of the American Ceramics Society* (submitted)	May 2003
1027	Riahi, D. N.	On flow of binary alloys during crystal growth—*Recent Research Development in Crystal Growth*, in press (2003)	May 2003
1028	Riahi, D. N.	On fluid dynamics during crystallization—*Recent Research Development in Fluid Dynamics*, in press (2003)	July 2003
1029	Fried, E., V. Korchagin, and R. E. Todres	Biaxial disclinated states in nematic elastomers—*Journal of Chemical Physics* **119**, 13170–13179 (2003)	July 2003
1030	Sharp, K. V., and R. J. Adrian	Transition from laminar to turbulent flow in liquid filled microtubes—*Physics of Fluids* (submitted)	July 2003
1031	Yoon, H. S., D. F. Hill, S. Balachandar, R. J. Adrian, and M. Y. Ha	Reynolds number scaling of flow in a Rushton turbine stirred tank: Part I—Mean flow, circular jet and tip vortex scaling—*Chemical Engineering Science* (submitted)	Aug. 2003
1032	Raju, R., S. Balachandar, D. F. Hill, and R. J. Adrian	Reynolds number scaling of flow in a Rushton turbine stirred tank: Part II—Eigen-decomposition of fluctuation—*Chemical Engineering Science* (submitted)	Aug. 2003
1033	Hill, K. M., G. Gioia, and V. V. Tota	Structure and kinematics in dense free-surface granular flow—*Physical Review Letters*, in press (2003)	Aug. 2003
1034	Fried, E., and S. Sellers	Free-energy density functions for nematic elastomers—*Journal of the Mechanics and Physics of Solids* (submitted)	Sept. 2003
1035	Kasimov, A. R., and D. S. Stewart	On the dynamics of self-sustained one-dimensional detonations: A numerical study in the shock-attached frame—*Physics of Fluids* (submitted)	Nov. 2003
1036	Fried, E., and B. C. Roy	Disclinations in a homogeneously deformed nematic elastomer—*Nature Materials* (submitted)	Nov. 2003
1037	Fried, E., and M. E. Gurtin	The unifying nature of the configurational force balance—*Mechanics of Material Forces* (P. Steinmann and G. A. Maugin, eds.), in press (2003)	Dec. 2003
1038	Panat, R., K. J. Hsia, and J. W. Oldham	Rumpling instability in thermal barrier systems under isothermal conditions in vacuum—*Philosophical Magazine* (submitted)	Dec. 2003